Received: 29 April 2020 | Revised: 12 November 2020 | Accepted: 4 January 2021

IET Renewable Power Generation

DOI: 10.1049/rpg2.12101

ORIGINAL RESEARCH PAPER

Interval optimization-based scheduling of interlinked power, gas, heat, and hydrogen systems

Nima Nasiri[1] | **Ahmad Sadeghi Yazdankhah**[1] | **Mohammad Amin Mirzaei**[2] | **Abdolah Loni**[3] | **Behnam Mohammadi-Ivatloo**[2,4] | **Kazem Zare**[2] | **Mousa Marzband**[5,6]

[1] Department of Electrical Engineering, Sahand University of Technology, Tabriz, Iran

[2] Faculty of Electrical and Computer Engineering, University of Tabriz, Tabriz, Iran

[3] Faculty of Mathematics Sciences and Computer, Allameh Tabataba'i University, Tehran, Iran

[4] Department of Energy Technology, Aalborg University, Aalborg, Denmark

[5] Northumbria University, Electrical Power and Control Systems Research Group, Newcastle upon Tyne, UK

[6] Center of Research Excellence in Renewable Energy and Power Systems, King Abdulaziz University, Jeddah, Saudi Arabia

Correspondence
Ahmad Sadeghi Yazdankhah, Department of Electrical Engineering, Sahand University of Technology, Tabriz, Iran.
Email: sadeghi@sut.ac.ir

Abstract

The combined heat and power (CHP) plant is one of the emerging technologies of gas-fired units, which plays an important role in reducing environmental pollutants and delivering high energy efficiency. Moreover, the hydrogen energy storage (HES) system with extra power storage from wind turbine via power to hydrogen technology allows the injection of stored energy into the power grid by reverse hydrogen to power services, offsetting in this way the uncertainty of wind power. Consequently, simultaneous usage of CHP and HES units not only makes the maximum use of wind power distribution but also increases flexibility and reduces the operating costs of the entire network. Therefore, this paper proposes an interval optimization technique for managing the uncertainty of wind power generation in the integrated electricity and natural gas (NG) networks considering CHP–HES. Moreover, to enhance the flexibility of the NG network, a linearized Taylor series-based model is proposed for modelling linepack of gas pipelines in the proposed scheduling framework that is formulated mixed-integer linear programming and solved using the Cplex solver. The obtained results indicate that the simultaneous use of CHP–HES in the day-ahead scheduling reduces the operating cost and increases the flexibility of the whole network.

1 | INTRODUCTION

The desire to provide safe, efficient, and sustainable energy calls for dramatic changes in energy networks. In line with this, with the technological advancement of multiple energy systems (MES) across a spectrum range of disciplines, it is possible to establish a physical connection between various energy networks such as electricity, natural gas (NG), hydrogen, and local heating. Such an initiative will lessen the barriers to traditional non-integrated networks. As a result, the entire energy supply chain in modern society has undergone a rapid transition to an integrated energy network. One of the most important technologies in the integration of energy networks is the combined heat and power (CHP) units. These units are utilized in industries to provide electricity and heat at the same time. The heat generated by the recovery of waste heat is obtained in the process of producing electrical energy. This method leads to a decrease in the cost of supplying electrical and heat demand, as well as reducing greenhouse gas emissions. Reports demonstrate that using CHP units instead of conventional production units results in gaining a maximum efficiency of up to 90% [1]. Also, CHP units reduce the emission of pollutants by 13–18% [2].

In recent years, many studies have been conducted on the coordination of integrated electricity and NG networks. The authors in [3] have investigated the impact of NG network constraints on the unit commitment (UC) in power grids. A mixed-integer linear programming (MILP) model has been considered in [4] to study the impact of applying the electric storage system to integrated electricity and NG systems with the aim of increasing system reliability and pressure control in NG network pipelines. In [5], a two-step multi-objective problem has been investigated on the unit's commitment of integrated electricity and gas networks, taking into consideration the flexible energy sources such as the power to gas (P2G) and demand response (DR) program, as well as high permeability level of the wind energy source. A coordinate-decomposition-based framework is proposed to study the optimization performance of integrated electricity and NG systems in [6]. In this framework, a robust distributed optimization model is presented based on the existing data to solve the problem of power system scheduling, considering wind energy uncertainty. A robust security-constrained UC model based on info-gap diction theory (IGDT) has been provided in [7]. Numerical analysis shows that flexible resources such as compressed air energy storage (CAES) and DR lead to a reduction in operating costs and management of wind power uncertainty. A stochastic day-ahead scheduling approach has been proposed for the hourly dispatch of power plants and deploys flexible ramping for the management of renewable energy sources in integrated electricity and NG networks [8]. The conducted research studies show that the real-time distribution of NG can directly affect the hourly distribution of deploying flexible ramping and the operating costs of networks. In [9], a market-clearing model constrained by the restrictions of the electricity and NG networks with a two-step stochastic unit commitment approach has been discussed considering the impact of CAES to increase network flexibility. A bi-level scheduling is suggested in [10] for integrated NG and electricity systems. The purpose of this bi-level problem is to minimize the costs of investing in wind farms, P2G equipment, NG storage units, as well as day-ahead market operating costs. The authors in [11] provided a context to evaluate the impact of different types of economic, environmental, security, and sustainability indicators on the integrated performance of integrated energy systems considering the constraints of electricity, NG, and district heating networks. In [12], to improve the system performance and optimize energy flow, a coordinated strategy has been proposed based on a non-probabilistic optimization model considering the DR program for integrated electricity and NG systems. The authors in [13] have investigated a non-linear scheduling problem for electricity and NG systems, where the uncertainty of the electricity price is managed by applying the IGDT method. In [14], a hybrid IGDT-stochastic approach for integrated power and NG systems has been presented to reduce the total operating costs of the integrated system and increase the permeability of wind turbines by applying P2G technology. In [15], a two-stage iterative-based algorithm for the interaction of integrated electricity and natural gas networks in the presence of the energy hub system under the approach of stochastic uncertainty is presented. A two-stage stochastic approach to the operation of integrated power and natural gas networks considering interconnected hubs is presented in [16]. Many researchers have been focused on the optimal operation of CHP units in heat- and power-based energy systems. The impact of CHPs in the UC problem has been analyzed in [17]. An IGDT approach has been presented to evaluate the profit-oriented strategy for CHP units in an electricity market [18]. A market-clearing model for integrated electricity and NG networks considering CHP and P2G technologies was provided in [19] to minimize the expected operating costs. In [20], a DC power flow has been utilized in the problem of energy pricing in electricity, NG, and heat networks in the presence of CHP units and limits of pollutant emissions. In [21], robust scheduling to optimize the performance of CHP with a demand response program aimed at reducing operating costs was presented. A unit commitment problem for CHP units with the aim of reducing pollutant emission was presented in [22]. In [23], a non-linear approach has been provided for optimizing photovoltaic heating systems and the CHP system with the aim of maximizing profits using a demand retrospective program. The authors in [24] have presented multi-objective scheduling for optimal performance of CHP system and energy storage systems (ESSs) in the presence of DR program with the goals of minimizing CHP operation costs and minimizing pollutant emission costs. In [25], mixed-integer non-linear programming was presented to optimize the day-ahead integrated electrical–water–heat systems to minimize the operating costs of the CHP and the fuel cost for freshwater. It also evaluates the impact of the hybrid vehicle and DR program on the target system.

Hydrogen energy storage (HES) technology plays a major role in strengthening the balance between generation and consumption of energy. Much research has been done on the optimal operation of HES technology, for example, the authors in [26] proposed the optimal scheduling for an intelligent parking lot (IPL) considering the demand response program and the uncertainty derived from the energy price of the upstream network. In [27], risk-averse stochastic exploitation of HES in the presence of the wind energy sources has been presented. In addition, the demand response program is considered utilizing a scenario-based stochastic approach. In [28], a stochastic UC problem has been modelled considering security constraints, HES system, and price-based DR program. In [29] a multi-objective approach to the optimal scheduling of hybrid renewable energy systems, including wind turbines, solar panels, fuel cells, electrolysis, hydrogen storage system, and electrical storage systems, is presented. The authors in [30] have proposed optimal stochastic scheduling to study the coordination impact of hydrogen storage systems, diesel generators, solar panels, water electrolyzer, fuel cell (FC), and electric vehicle. The results show that most of the solar energy is consumed by hydrogen storage and reduces the operating costs. The authors in [31] have proposed a stochastic approach in IPL integrated with the HES to minimize the cost of purchasing energy from the upstream grid using a particle swarm optimization (PSO) algorithm. In [32], an energy management system for optimal operation of photovoltaic, battery, and hydrogen storage systems using PSO algorithm is presented. In [33], optimal scenario-based management was presented for a grid-connected microgrid with various RESs such as FC, wind turbine, microturbine, and electrical storage system to improve energy management and reduce microgrid costs.

To the best knowledge of the authors, none of the reviewed works have examined the synergy between the HES system and the integrated electricity and NG networks in the presence of the CHP unit and linepack flexibility. The main gaps in the reviewed literature can be summarized as follows:

- In some works, for example, [3–9, 11–14], the problem of optimal scheduling of integrated electricity and NG systems without considering the linepack system has been investigated. The existence of linepack system in natural gas networks is very useful and increases the flexibility of NG systems and generation units, especially in critical times of the NG network. In addition, the linepack system reduces the total operating costs of the integrated electricity and NG system.

- In some studies, for example, [16–19, 21–24], the problem of optimal generation scheduling of CHP units has been evaluated without considering the constraints of the NG network. Constraints of the NG network have a significant impact on the commitment of units in the power grid. Ignoring the constraints of the NG network in scheduling the commitment of units leads to unrealistic and careless results.
- In some literature, for example, [25, 26, 28–34], the problem of optimal scheduling of HES systems without considering the constraints of the power and NG grids has been investigated. Ignoring such constraints cannot completely describe the benefits of HES in optimal scheduling of the integrated energy systems.

To cover these gaps, here, an interval optimization technique is proposed for the day-ahead scheduling of integrated electricity and NG networks considering HES and CHP units. In addition, the linepack technology is applied to increase the flexibility of the power and NG system. The main contributions of this paper are as follows:

- Investigating the impact of the HES system on the day-ahead scheduling of integrated electricity and NG networks aiming to minimize the cost of operating costs of both networks with CHP unit and wind energy sources.
- Performing an interval optimization technique to handle the uncertainty of wind energy production and its impact on the operating costs of the whole network.
- The proposed interval approach is formulated as a multi-objective optimization problem in which the average cost and cost deviation are minimized simultaneously.
- Evaluation of gas system flexibility equipped with linepack technology on power dispatch of gas-fired and non-gas-fired units in critical times of NG network.

The remaining is organized as follows: Section 2 introduces HES. Section 3 presents the problem description and formulation. Section 4 revolves around an interval optimization technique to estimate the existing uncertainties. Section 4 describes the results and discussion regarding the proposed model. Ultimately, Section 5 concludes the paper.

2 | HYDROGEN STORAGE TECHNOLOGY

The HES technology, in addition to emissions reduction, can play an important role in securing network demand–supply. As shown in Figure 1, HES technology converts electrical energy into hydrogen by electrolyzer in periods of off-peak and high wind energy generation, then stores it in a hydrogen storage tank. In this way, during periods of on-peak and low wind energy production, the stored energy can be converted to electric power by the fuel cell and is injected into the grid. This

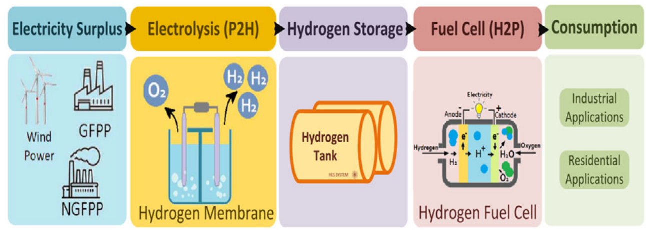

FIGURE 1 HES system performance diagram

operation, while optimally managing wind uncertainty, can play an important role in reducing the generation power of expensive power units. A unique feature of HES compared to other ESSs is that it can be used in hydrogen-dependent industries or injected into the NG network for residential gas consumers [24].

3 | PROBLEM DESCRIPTION AND FORMULATION

In this research, it is assumed that the optimal scheduling of the integrated energy system is the responsibility of a central system operator (CSO). The CSO holds comprehensive information on the operation of the power grid and NG network. Based on the available data, the CSO performs the optimal scheduling of the integrated system in a day-ahead time horizon. As illustrated in Figure 2, three types of power generating units are considered in this study: (a) CHP unit, (b) gas-fired power plant (GFPP), and (c) non-gas-fired power plant (NGFPP). Physically, power and NG networks are connected via CHP and GFPP. In this research, linepack technology has been used to increase system reliability and pressure constraint security in NG pipelines. Linepack technology enhances the flexibility of the NG system by storing some of the gas in the network pipelines. In addition, we have used HES technology to increase the security of supply and demand in the power grid as well as to absorb the wind power overcapacity.

3.1 | Objective function

The objective in problem formulation is to minimize the costs of (i) NGFPP cost and startup/shutdown of NGFPP, (ii) NG producers, (iii) HES costs.

$$\min \sum_t \left\{ \begin{array}{l} \sum\limits_{i \in CU} \left(FC_{i,t} + SU_{i,t} + SD_{i,t} \right) \\ + \sum\limits_{sp} \gamma_{sp}^{gas} V_{sp,t} + \sum\limits_{h} \rho_h^{HES} P_{h,t}^{H2P} \end{array} \right\} \tag{1}$$

The first term of Equation (1) concerns the operating cost and startup/shutdown of power plants resulting from the electricity generation cost of NGFPP. The second term deals with the producer costs of NG (NG wells). The third term is the cost of HES in discharge mode. The various sets of constraints are presented below.

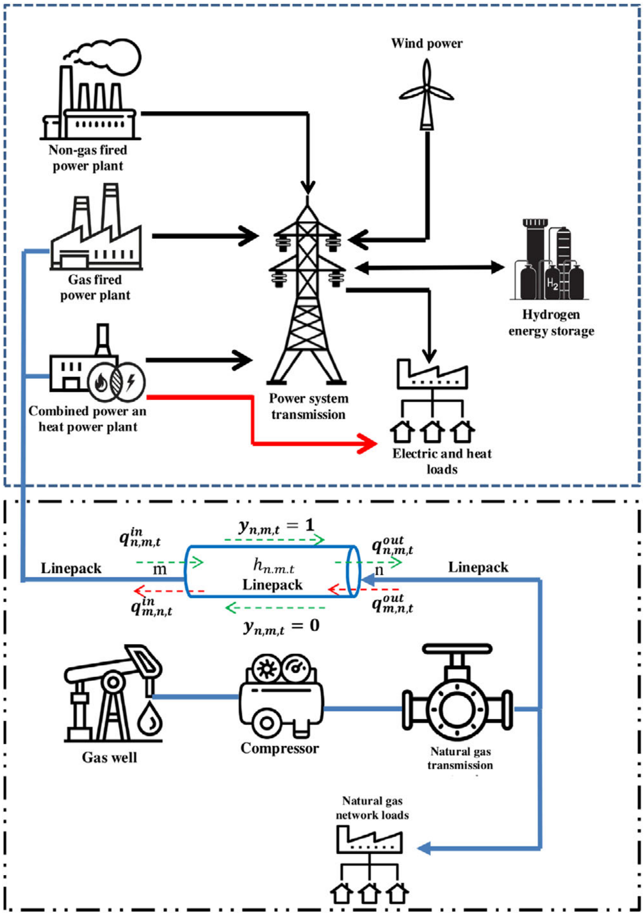

FIGURE 2 Integrated power and NG networks considering wind–HES–CHP

3.2 | Generating unit constraints

The constraint in Equation (2) relates to the limitation of power units generation, and Equations (3) and (4) are related to the startup/shutdown cost of NGFPP. Furthermore, Equations (5) and (6) revolve around the startup/shutdown cost of GFPP, and Equations (7) and (8) set the startup/shutdown modes of all units. Equations (9) and (10) are related to the rate of ramp-up and ramp-down in the units' generation power.The linearized constraints in Equations (11) and (12) represent the number of hours required by generation unit i startup and shutdown at the beginning of the study horizon. Equation (13) applies the minimum ON time requirement if generation unit i is on-line at the beginning of the study horizon. Equation (14) applies the minimum ON time requirement for all consecutive sets of hours of cardinality T_i^{on}. Equation (15) applies the minimum ON time requirement for the final T_i^{on} hours of the study horizon. Equation (16) applies the minimum OFF time requirement if generation unit i is off-line at the beginning of the study horizon. Equation (17) applies the minimum OFF time requirement for all consecutive sets of hours of cardinality T_i^{off}. Equation (18)applies the minimum OFF time requirement for the final T_i^{off} hours of the study horizon.

$$P_i^{Min} I_{i,t} \le P_{i,t} \le P_i^{Max} I_{i,t} \quad \forall i \in \{CU, GU\}, \forall t \tag{2}$$

$$SU_{i,t} \ge C_i^{SU} y_{i,t} \quad \forall i \in CU, \forall t \tag{3}$$

$$SD_{i,t} \ge C_i^{SD} z_{i,t} \quad \forall i \in CU, \forall t \tag{4}$$

$$GSU_{i,t} \ge C_i^{GSU} y_{i,t} \quad \forall i \in GU, \forall t \tag{5}$$

$$GSD_{i,t} \ge C_i^{GSD} z_{i,t} \quad \forall i \in GU, \forall t \tag{6}$$

$$y_{i,t} - z_{i,t} = I_{i,t-1} - I_{i,t} \quad \forall i, \forall t \tag{7}$$

$$y_{i,t} + z_{i,t} \le 1 \quad \forall i, \forall t \tag{8}$$

$$P_{i,t} - P_{i,t-1} \le (1 - y_{i,t}) R_i^{UP} + y_{i,t} P_i^{Min} \quad \forall i, \forall t \tag{9}$$

$$P_{i,t-1} - P_{i,t} \le (1 - z_{i,t}) R_i^{DN} + z_{i,t} P_i^{Min} \quad \forall i, \forall t \tag{10}$$

$$L_i^{on} = \min\left\{ T, (T_i^{on} - T_{i,0}^{on}) I_{i,0} \right\} \tag{11}$$

$$L_i^{off} = \min\left\{ T, (T_i^{off} - T_{i,0}^{off})(1 - I_{i,0}) \right\} \tag{12}$$

$$\sum_{t \in L_i^{on}} (1 - I_{i,t}) = 0 \quad \forall i \tag{13}$$

$$\sum_{t=r}^{t+T_i^{on}-1} I_{i,r} \ge T_i^{on} (I_{i,t} - I_{i,t-1}) \quad \forall i, \quad \forall t \in \left[L_i^{on} + 1, \ldots, T - T_i^{on} + 1 \right] \tag{14}$$

$$\sum_{t=r}^{T} (I_{i,r} - (I_{i,t} - I_{i,t-1})) \ge 0 \quad \forall i, \forall t \in \left[T - T_i^{on} + 2, \ldots, T \right] \tag{15}$$

$$\sum_{t \in L_i^{off}} I_{i,t} = 0 \quad \forall i \tag{16}$$

$$\sum_{t=r}^{t+T_i^{off}-1} (1 - I_{i,r}) \ge T_i^{off} (I_{i,t-1} - I_{i,t}) \quad \forall i, \forall t \in \left[L_i^{off} + 1, \ldots, T - T_i^{off} + 1 \right] \tag{17}$$

$$\sum_{t=r}^{T} (1 - I_{i,r} - (I_{i,t-1} - I_{i,t})) \ge 0 \quad \forall i, \forall t \in \left[T - T_i^{off} + 2, \ldots, T \right] \tag{18}$$

3.3 | Constraints of electricity grid

Equation (19) indicates the constraint of electricity grid balance and Equation (20) describes the limitation of power flow on lines. Further, Equation (21) concerns DC power flow in the power grid and Equation (22) defines the phase angle of the slack bus, also Equation (23) relates to the production constraint of the wind power plant.

$$\sum_{j\in Tr} f_{b,j,t} + \sum_{h\in A_b^{HES}} P_{h,t}^{P2H} + P_{b,t}^{Load}$$

$$= \sum_{i\in A_b^i} P_{i,t} + \sum_{w\in A_b^w} PW_{w,t} + \sum_{h\in A_b^{HES}} P_{h,t}^{H2P} \quad \forall b, \forall t \quad (19)$$

$$-f_b^{Max} \le f_{b,j,t} \le f_b^{Max} \quad \forall (b,j) \in Tr, \forall t \quad (20)$$

$$f_{b,j,t} = (\delta_{b,t} - \delta_{j,t})/X_L \quad \forall (b,j) \in Tr, \forall t \quad (21)$$

$$\delta_{ref,t} = 0 \quad \forall t \quad (22)$$

$$0 \le PW_{w,t} \le PW_w^{\max} \quad \forall w, \forall t \quad (23)$$

3.4 | Constraints of CHP unit

The day-ahead scheduling constraints for CHP system are presented Equations (24) and (25).The amount of electric power and heat energy production in CHP unit is interdependent and is calculated by the feasible CHP operation region. As shown in Figure 4, the operating area of a CHP unit can be described by a polyhedron characteristic. Equations (24) and (25), respectively, show how CHP generates electricity and heat depending on the characteristic of combined points in the CHP operating area. The non-negative coefficient of a_t^k, constrained by (26) and (27), expresses the CHP unit commitment. In addition, Equation (28) demonstrates the balance of heating energy that is fully supplied by the CHP [35].

$$P_{i,t} = \sum_{k=1}^{NK} \alpha_t^k P^k \quad \forall i \in CHP, \forall t \quad (24)$$

$$H_{i,t} = \sum_{k=1}^{NK} \alpha_t^k Q^k \quad \forall i \in CHP, \forall t \quad (25)$$

$$\sum_{k=1}^{NK} \alpha_t^k = I_{i,t} \quad \forall i \in CHP, \forall t \quad (26)$$

$$0 \le \alpha_t^k \le 1 \quad \forall i \in CHP, \forall t \quad (27)$$

$$\sum_{i=1} H_{i,t} = H_t^{load} \quad \forall i \in CHP, \forall t \quad (28)$$

3.5 | The constraints of nodes and NG flow

The pressure constraints of NG network nodes are given in Equation (29). According to Equation (30), NG flow can be expressed as a function of the square of pressure and the characteristics of pipe such as length, diameter, and friction coefficient. Equation (30) is referred to as the general flow [36] that can be approximated by Weymouth equations under certain conditions. This model, given the function of sgn (mentioned in Equation (31)), allows the flow to be bidirectional. It is important to mention that Equation (30) is non-convex in addition to being non-linear.

$$Pr_n^{Min} \le Pr_{n,t} \le Pr_n^{Max} \quad (29)$$

$$q_{n,m,t} = sgn(Pr_n, Pr_m) K_{n,m}^f \sqrt{Pr_{n,t}^2 - Pr_{m,t}^2} \quad \forall n, \forall t \quad (30)$$

$$\mathrm{sgn}(\mathrm{Pr}_n, \mathrm{Pr}_m) = \begin{cases} 1, & \mathrm{Pr}_n \ge \mathrm{Pr}_m \\ -1, & \mathrm{Pr}_n \le \mathrm{Pr}_m \end{cases} \quad \forall (n,m) \in z \quad (31)$$

The non-linearity and non-convexity of the gas flow equation make the pricing of NG more difficult. Therefore, we use an outer approximation approach based on the Taylor series at the fixed pressure points to linearize the Weymouth equation [36] and present a globally optimal solution.

$$q_{n,m,t} \le \frac{K_{n,m}^f PR_{n,u}}{\sqrt{PR_{n,u}^2 - PR_{m,u}^2}} \mathrm{Pr}_{n,t} - \frac{K_{n,m}^f PR_{m,u}}{\sqrt{PR_{n,u}^2 - PR_{m,u}^2}} \mathrm{Pr}_{m,t} \quad (32)$$

$$\forall (n,m) \in z, \forall t$$

Here, u is set of pressure fixed points ($\mathrm{PR}_{n,u}$, $\mathrm{PR}_{m,u}$) [37]. However, the limitation of the gas flow is approximated by Equation (32). The sgn function is ignored in (31) because of non-linearity. Hence, to guarantee the bidirectional flow of gas in the pipeline, defining an equation is vital. Consequently, to this end, inequalities Equations (33)–(36) are used to ensure the bidirectional flow of the network [36].

$$q_{n,m,t} = q_{n,m,t}^+ - q_{n,m,t}^- \quad (33)$$

$$q_{n,m,t}^- = M(1 - y_{n,m,t}) \quad \forall (n,m) \in z, \forall t \quad (34)$$

$$q_{n,m,t}^+ = M y_{n,m,t} \quad \forall (n,m) \in z, \forall t \quad (35)$$

$$y_{n,m,t} \in \{1, 0\} \quad \forall (n,m) \in z, \forall t \quad (36)$$

where $q_{(n,m,t)}^+$ denotes the gas flow in the pipeline from node n to m and vice versa for $q_{(n,m,t)}^-$. The parameter M is a large constant number and Equations (33) fulfills the function of sgn. Equations (34) and (35) ensure that only one of the two variables $q_{(n,m,t)}^-$, $q_{(n,m,t)}^+$ is non-zero. In addition to the above mentioned limitations, the following inequalities should be defined [36]:

$$q_{n,m,t}^+ \le \frac{K_{n,m}^f PR_{n,u} Pr_{n,t}}{\sqrt{PR_{n,u}^2 - PR_{m,u}^2}} - \frac{K_{n,m}^f PR_{m,u} Pr_{m,t}}{\sqrt{PR_{n,u}^2 - PR_{m,u}^2}}$$

$$+M(1-y_{n,m,t})\ \left\langle \forall(n,m)\in z \mid m<n\right\rangle,\forall u,\forall t \quad (37)$$

$$q^{-}_{n,m,t} \le \frac{K^{f}_{n,m}\, PR_{m,u}\, Pr_{m,t}}{\sqrt{PR^{2}_{m,u}-PR^{2}_{n,u}}} - \frac{K^{f}_{n,m}\, PR_{n,u}\, Pr_{n,t}}{\sqrt{PR^{2}_{m,u}-PR^{2}_{n,u}}} \quad (38)$$

$$+M(y_{n,m,t})\ \left\langle \forall(n,m)\in z \mid m>n\right\rangle,\forall u,\forall t \quad (38)$$

The linear Equations (37) and (38) state the direction of gas flow, specified by binary variables. In addition, two positive variables $q^{+}_{(n,m,t)}$, $q^{-}_{(n,m,t)}$ are determined for the flexibility of linepacks to specify inflow and outflow [36].

$$q^{+}_{n,m,t} = \frac{q^{in}_{n,m,t}-q^{out}_{n,m,t}}{2}\quad \forall(n,m)\in z,\forall t \quad (39)$$

$$q^{-}_{n,m,t} = \frac{q^{in}_{m,n,t}-q^{out}_{m,n,t}}{2}\quad \forall(n,m)\in z,\forall t \quad (40)$$

One of the unique features of NG networks is linepack that can serve as temporary storage (an economical way to store energy). The linepack system indicates the ability to store a certain amount of NG in the pipeline and is very important for short-term NG network operation [36].

The linepack system indicates the ability to store a certain amount of NG in the pipeline and is very important for short-term NG network operation.

$$h_{n,m,t} = K^{f}_{n,m}\frac{Pr_{n,t}+Pr_{m,t}}{2}\quad \forall(n,m)\in z,\forall t \quad (41)$$

$$h_{n,m,t} = h_{n,m,t-1} + q^{in}_{n,m,t} - q^{out}_{n,m,t}\quad \forall(n,m)\in z,\forall t\ge 1 \quad (42)$$

$$h_{n,m,t} = h_{n,m,0} + q^{in}_{n,m,t} - q^{out}_{n,m,t}\quad \forall(n,m)\in z,\forall t = 1 \quad (43)$$

$$h_{n,m,s,t} \le h_{n,m,s,0}\quad \forall(n,m)\in z,\forall t \quad (44)$$

Equation (41) shows that the linepack system is directly related to the average pressure in the pipeline. Therefore, increasing the pressure in a pipeline node leads to an increase in the linepack and vice versa. Moreover, Equations (42) and (43) show that the linepack, in addition to, Equation (39) is equal to the difference between the pipeline's inflow and outflow. Furthermore, the initial value of linepack is represented by Equation (44).

3.6 | Other technical constraints of the NG network

The constraint in Equation (45) relates to the limitation of gas generated by NG wells, whereas, Equation (46) specifies the energy balance in NG production and consumption. Furthermore, Equation (47) and (48) indicate the coupling constraints of electricity and NG networks through GFPP and CHP unit.

$$V^{Min}_{sp} \le V_{sp,t} \le V^{Max}_{sp}\quad \forall sp,\forall t \quad (45)$$

$$\sum_{sp\in A^{sp}_{n}} V_{sp,t} - \sum_{l\in A^{l}_{n}} L_{l,t} - \sum_{m\in z}(q^{in}_{n,m,t}-q^{out}_{m,n,t}) = 0\quad \forall n,\forall t \quad (46)$$

$$L_{l,t} = \sum_{i\in GU}\beta_i P_{i,t}\quad \forall l,\forall t \quad (47)$$

$$L_{l,t} = \sum_{i\in CHP}\gamma_P P_{i,t}+\gamma_H H_{i,t}\quad \forall l,\forall t \quad (48)$$

3.7 | The constraints of HES system

The constraints of HES performance are presented in the form of Equations (49)–(55). The amount of energy stored in the HES is given by Equation (49) and it depends on the energy stored in the previous time. The constraint in Equation (50) represents the upper and lower bounds of HES. Further, Equation (51) indicates that the initial and final values of HES are equal and Equation (52) is known as the applied hydrogen in other applications. In addition, Equations (53) and (54) are related to the charge and discharge limits, and Equation (55) prevents simultaneous charge and discharge [26].

$$A_{h,t} = A_{h,t-1} + \eta^{P2H}_{h} P^{P2H}_{h,t} - \frac{P^{H2P}_{h,t}}{\eta^{H2P}_{h}} - M_{h,t}\quad \forall h,\forall t \quad (49)$$

$$A^{Min}_{h} \le A_{h,t} \le A^{Max}_{h}\quad \forall h,\forall t \quad (50)$$

$$A_{h,t=0} = A_{h,24} = A_{h,in}\quad \forall h,\forall t \quad (51)$$

$$0 \le M_{h,t} \le M^{Max}_{h}\quad \forall h,\forall t \quad (52)$$

$$P^{P2H}_{h,Min} I^{P2H}_{h,t} \le P^{P2H}_{h,t} \le P^{P2H}_{h,Max} I^{P2H}_{h,t}\quad \forall h,\forall t \quad (53)$$

$$P^{H2P}_{h,Min} I^{H2P}_{h,t} \le P^{H2P}_{h,t} \le P^{H2P}_{h,Max} I^{H2P}_{h,t}\quad \forall h,\forall t \quad (54)$$

$$I^{P2H}_{h,t} + I^{H2P}_{h,t} \le 1\quad \forall h,\forall t \quad (55)$$

3.8 | Interval optimization technique

Each optimization problem can be mapped onto a standard optimization problem. Thus, considering the constraints and uncertainty parameter ρ, a standard optimization problem is as follows:

$$Min\ f(x, u, \rho) \tag{56}$$

$$h(x, u, \rho) \le 0 \tag{57}$$

$$g(x, u, \rho) \le 0 \tag{58}$$

According to interval optimization technique, uncertainty parameter (as an interval variable) has an upper and lower bound $[U^{min}, U^{max}]$. All constraints and objective function are examined with upper and lower boundary conditions, and can be expressed as in Equations (59) and (60):

$$f(x)^- = Min\ f(x) \tag{59}$$

$$f(x)^+ = Max\ f(x) \tag{60}$$

Given that uncertainty parameter fluctuations affect the objective function, these changes are expressed as an interval. Thus, instead of minimizing an objective function based on the interval, a two-objective model including the costs of deviation and average is generated, as stated by Equations (61)–(63). It is worth noting that $f(X)^W$ and $f(X)^M$ are average and deviation costs, respectively.

$$\min f(x) = \min(f(x)^M, f(x)^W) \tag{61}$$

$$f(x)^M = \frac{f(x)^+ + f(x)^-}{2} \tag{62}$$

$$f(x)^W = \frac{f(x)^+ - f(x)^-}{2} \tag{63}$$

Fuzzy and ϵ approaches are used to solve multi-objective problems [38]. In the first step, the global minimum and maximum of each objective function are calculated. In what follows, the objective function with higher priority is considered as the main objective function and other objective function as the constraint for the main function.

Therefore, the value of second objective function belongs to the open interval $f^M_{min}(x)$, $f^M_{max}(x)$. As a result, the main objective function is modified accordingly and Pareto table is created. Finally, in the obtained Pareto table, the per-unit values of both objective functions are calculated in each iteration and then the obtained minimum is selected. This section is carried out by Fuzzy satisfaction method, which is expressed by Equations (64)–(67) [39].

$$f(x)^M_{P.U} = \frac{f(x)^M + f^M_{\max}(x)}{f^M_{\min}(x) + f^M_{\max}(x)} \tag{64}$$

$$f(x)^W_{P.U} = \frac{f(x)^W + f^W_{\max}(x)}{f^W_{\min}(x) + f^W_{\max}(x)} \tag{65}$$

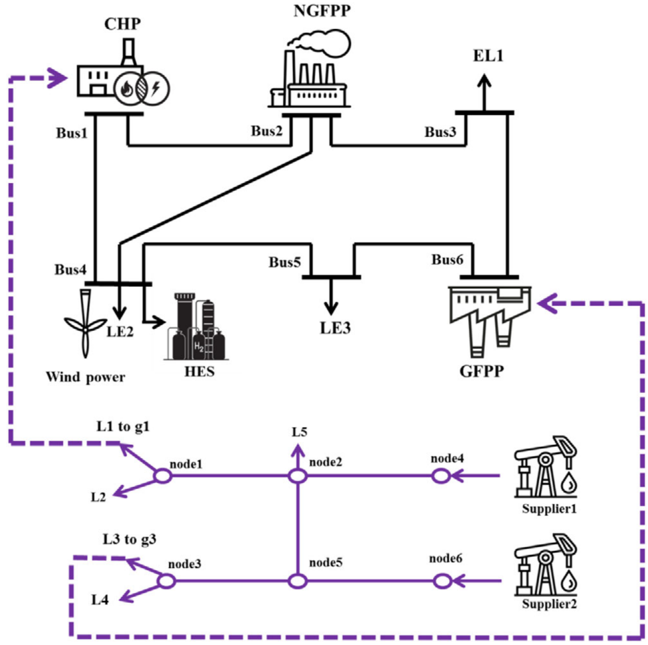

FIGURE 3 Modified 6-bus power grid with 6-node NG network

$$f^n = \min(f^n_1, \dots, f^n_N) \tag{66}$$

$$f^n = \min(f^n_1, \dots, f^n_N) \tag{67}$$

4 | RESULTS AND DISCUSSION

4.1 | Case study (CS)

The proposed scheduling problem is formulated as MILP problem in GAMS environment using the CPLEX standard solver. Here, the proposed model is simulated by an IEEE 6-bus standard system for the electricity grid with a 6-node NG network. As illustrated in Figure 3, the case study includes two distinct parts as (i) **The electricity grid**. The modified 6-bus electricity grid comprises a GFPP, a CHP unit, and a NGFPP. In addition, the 6-bus system includes seven transmission lines and three electrical loads. The characteristics of units, buses, transmission lines, and load distribution are provided in [40]. The CHP unit, the GFPP, and the NGFPP are, respectively, located at buses 1, 6, and 2. (ii) **The NG network**. The 6-node NG network consists of five pipelines, two gas suppliers, and five NG loads. The characteristics of NG wells, pipelines, and linepack are provided in [40]. In addition, there is a wind production unit and a HES on the fifth bus.

The characteristic of CHP feasible operation region is provided in Figure 4 [19]. The energy consumption coefficients of CHP unit for energy production of electrical and heat are 2.40 and 0.3 Kcf/MWh, respectively [20]. The parameters and characteristics of the HES system can be obtained from [40]. The gas load demand of the 6-node NG network and local heat demand have been specified in Figure 5.

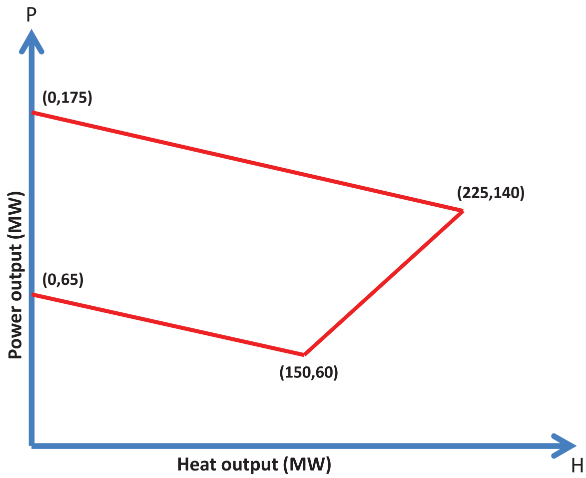

FIGURE 4 Operation area of the CHP unit

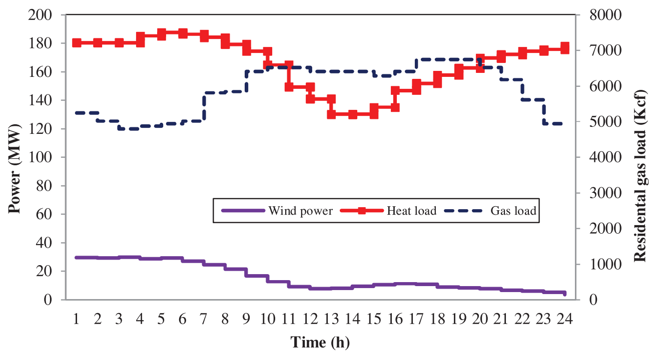

FIGURE 5 Total heat and NG demand curves

To show the performance of the provided model, the case study is analyzed in the form of three cases as follows:

Case study 1 (CS1): Evaluating the flexibility of NG equipped with linepack technology on day-ahead scheduling of hybrid energy networks

Figure 6 shows the hourly scheduling of UC compared to the residential load of NG network. As can be seen from Figure 6, the low-cost CHP unit is committed in the 24-h period to supply power and heat demands. The expensive NGFPP commits to distribute electricity only when the residential load of NG network increases. According to the comparison between NGFPP and the residential load of the NG network, the maximum output capacity of NGFPP is at the peak hour of the NG network, from $t = 16$ to $t = 19$. Also, the GFPP with a maximum capacity of 20 MW as the second-highest priority supplier enters the circuit from 10 to 24 h. The total operating cost in CS1 is equal to \$397,425.43. Of these, the production costs of GFPP and NGFPP are, respectively, equal to \$391,385.01 and \$6,040.42.

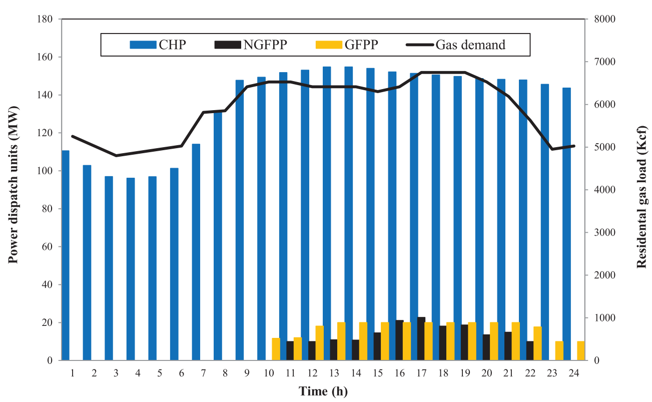

FIGURE 6 Hourly dispatch of units

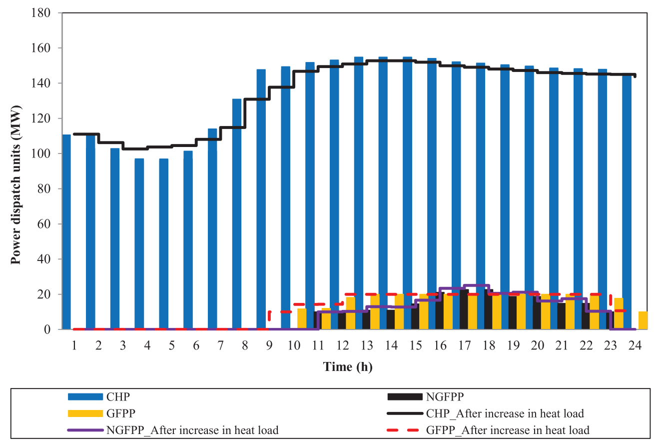

FIGURE 7 Comparison between hourly dispatch of units after 10% increase in district heat load

The effect of a 10% increase in local heating load on UC is illustrated in Figure 7. It is obvious that the capacity of the CHP unit has been decreased by 0.28%, while the NGFPP unit load increased by 12.42%. Also, the GFPP unit capacity raised by 7.62%. The total operating cost increased to \$398,886.49 after raising the local heating load by 10%. Of this amount, the production cost of the GFPP unit is \$392,136.17, and the electricity production cost of the NGFPP unit is \$6,750.33.

One of the most effective technologies utilized in NG networks is the linepack system. It increases the flexibility of the network by storing a certain amount of NG in the pipeline. According to Equation (41), it is obvious that the linepack system has a direct relationship with average pressure in the pipelines of the NG network. For this reason, increasing pressure on pipelines in an NG network is the same as increasing the linepack and vice versa. This reasoning can be seen from the obtained results in Figure 8. Moreover, the pressure and linepack changes in the pipeline (P1) have been compared in Figure 9, confirming the pointed out reasoning.

Figure 9 presents a comparison between changes in line pressure level and storage and discharge level in the pipeline P1. As shown in Figure 9, at times when the pressure is increasing at node 1, the linepack system starts to store NG energy. Moreover, at times of pressure drop, the pipeline of the NG network supplies the stored energy to the network.

In this section, the impact of linepack flexibility on the hourly dispatch of units in critical times is investigated. As a result, we increase the residential load on the NG network by up to 35%. In Figure 10, a comparison is made between the hourly scheduling of UCs in the presence of linepack and without linepack

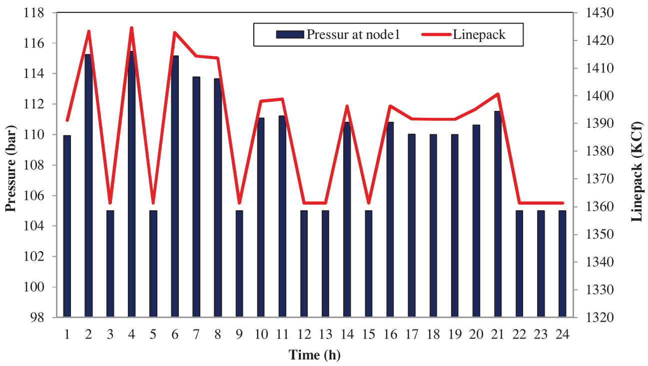

FIGURE 8 Comparison between linepack and pipeline pressure in the NG network

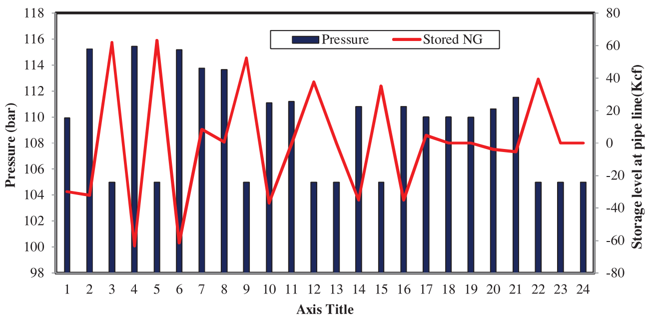

FIGURE 9 Comparison between storage level and pipeline pressure in the NG network

technology. As can be seen from Figure 10, when the NG system is equipped with linepack technology, it prevents excessive reduction of CHP unit at critical times. In addition, when the NG system is linepack technology, it prevents the excessive generation of expensive NGFPP at critical times. For this reason, linepack technology increases the reliability and flexibility of the integrated electricity and NG system. Also, according to Table 1, it can be seen that in addition to increasing the flexibility of the system, linepack technology reduces the operating costs of the integrated electricity and NG networks.

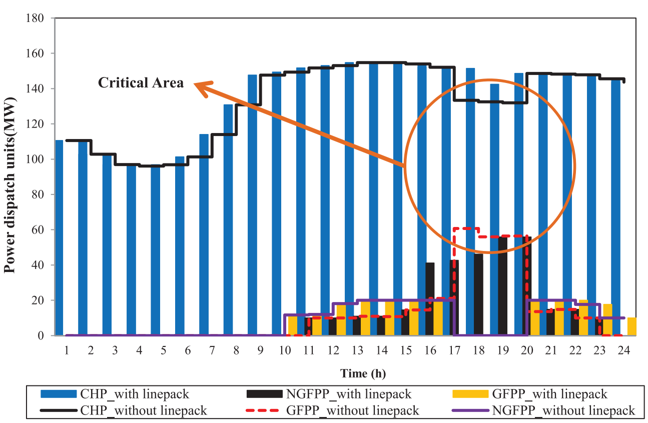

FIGURE 10 Hourly dispatch of units with/without considering linepack

TABLE 1 Compare operating costs with/without linepack technology

	With linepack under a 35% increase in forecasted gas load	Without linepack under a 35% increase in forecasted gas load
Total operation cost ($)	541,661.08	543,891.89
GFPP cost ($)	534,033.22	535,893.66
NGFPP cost ($)	7,627.85	7,998.22

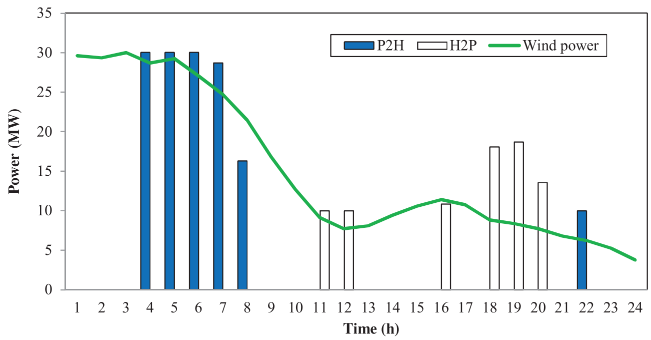

FIGURE 11 Hourly power stored and generated through HES system for CS2

Case study 2 (CS2): Evaluation of the impact of the HES system on day-ahead scheduling of hybrid energy networks

In this case, the impact of the HES system on the day-ahead scheduling of integrated electricity and NG networks is examined. As depicted in Figure 11, the HES system stores electricity at low-cost and during off-peak hours from $t = 4$ to $t = 8$. This is done by converting the electricity to hydrogen by power to hydrogen (P2H) technology and storing it in a hydrogen tank. Thus, the stored hydrogen in peak hours from $t = 15$ to $t = 20$ provides electricity to the network by hydrogen to power (H2P) technology. Figure 12 shows the effect of the HES system on UC. In addition, Figure 12 indicates the comparison between CS1 and CS2. The low-cost CHP unit commits to distribute electricity throughout the time period.

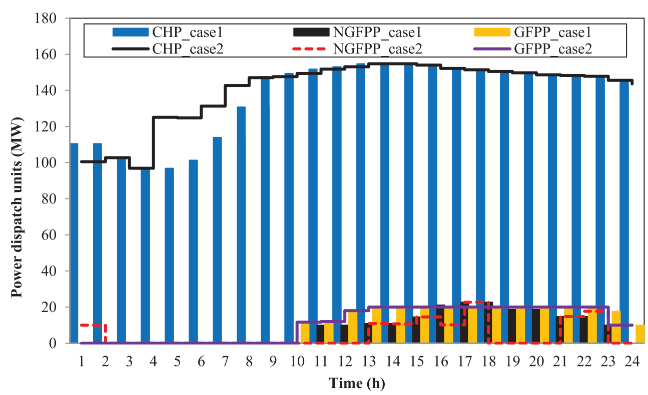

FIGURE 12 Hourly dispatch of Units for CS2

TABLE 2 Comparison of operating costs obtained for CS1 and CS2

	CS1	CS1	CS2
	Before increasing the heat load by 10%	After increasing the heat load by 10%	
Total operation cost ($)	397,425.4	398,886.5	395,623.7
(GFPP and CHP) cost ($)	391,385	392,136.2	392,263.6
NGFPP cost ($)	6040.423	6750.33	3253.587
Average cost ($)	397,522.80	398,814.2	395,703.8
Deviation cost ($)	1372.065	1331.934	1405.458

TABLE 3 Pareto solutions under forecasted heat load without HES

#	Average cost ($)	Deviation cost ($)	ϕ_1(p.u)	ϕ_2(p.u)	Min
1	397,522.8	1372.065	1	0	0
2	397,611	1283.865	0.9	0.1	0.1
3	397,699.2	1195.665	0.8	0.2	0.2
4	397,787.4	1107.465	0.7	0.3	0.3
5	397,875.6	1019.265	0.6	0.4	0.4
6	397,963.8	931.0651	0.5	0.5	0.5
7	398,052	842.8651	0.4	0.6	0.4
8	398,140.2	754.6651	0.3	0.7	0.3
9	398,228.4	666.4651	0.2	0.8	0.2
10	398,316.6	578.2651	0.1	0.9	0.1
11	398,404.8	490.0651	0	1	0

According to the comparison, the electricity dispatch of the CHP unit in the early and low-cost hours due to HES storage is significantly increased compared to CS1. The generation of the expensive NGFPP is abruptly reduced due to the discharge of HES between 12 and 22 h, reaching zero even at several hours. In this regard, the status of the GFPP unit's commitment is decreased in a few hours in comparison with CS1. The total operating cost for CS2 is $395,623.74. The generation cost of GFPP is $392,263.56, and the electricity production cost of NGFPP is equal to $3,253.59. The operating costs of the two case studies are compared in Table 2.

Case study 3 (CS3): Interval-based robust optimization of hybrid energy networks in the presence of HES

The optimal Pareto results for the day-ahead scheduling of integrated electricity and NG systems without considering HES technology are shown in Table 3. The average cost compared to the deterministic case increased by 0.11%, and the cost deviation decreased by 32.14%. Pareto optimal results for day-ahead scheduling of integrated electricity and NG systems (without considering of HES technology) and with a 10% increase in heat load are shown in Table 4. The average cost amount and deviation are, respectively, increased by 0.11% and 32.14% compared to the deterministic case. The optimal Pareto results for the day-ahead scheduling of integrated electricity and NG systems considering HES technology are shown in Table 5. The average

TABLE 4 Pareto solutions under a 10% increase in heat load without HES

#	Average cost ($)	Deviation cost ($)	ϕ_1(p.u)	ϕ_2(p.u)	Min
1	398,814.2	1331.934	1	0	0
2	398,902.4	1243.734	0.9	0.1	0.1
3	398,990.6	1155.534	0.8	0.2	0.2
4	399,078.8	1067.334	0.7	0.3	0.3
5	399,167	979.1339	0.6	0.4	0.4
6	399,255.2	890.9339	0.5	0.5	0.5
7	399,343.4	802.7339	0.4	0.6	0.4
8	399,431.6	714.5339	0.3	0.7	0.3
9	399,519.8	626.3339	0.2	0.8	0.2
10	399,608	538.1339	0.1	0.9	0.1
11	399,696.2	449.9339	0	1	0

TABLE 5 Pareto solutions under forecasted heat load with HES

#	Average cost ($)	Deviation cost ($)	ϕ_1(p.u)	ϕ_2(p.u)	Min
1	395,703.8	1405.458	1	0	0
2	395,792	1317.258	0.9	0.1	0.1
3	395,880.2	1229.058	0.8	0.2	0.2
4	395,968.4	1140.858	0.7	0.3	0.3
5	396,056.6	1052.658	0.6	0.4	0.4
6	396,144.8	964.4577	0.5	0.5	0.5
7	396,233	876.2577	0.4	0.6	0.4
8	396,321.2	788.0577	0.3	0.7	0.3
9	396,409.4	699.8577	0.2	0.8	0.2
10	396,497.6	611.6577	0.1	0.9	0.1
11	396,585.8	523.4577	0	1	0

cost amount and deviation, in this case, increase by 0.11% and 32.14%, respectively. From the analysis obtained from Tables 3–5, it can be concluded that, by reducing the cost deviation, the CSO incurs a high average operating cost, which in fact results in a more robust approach to the uncertainty of wind power.

5 | CONCLUSION

This paper presented optimal day-ahead scheduling for integrated wind–HES–CHP systems. In this study, linepack technology was applied to increase the flexibility and reliability of the NG system. According to results, it is observed that increasing the heating load by 10% raises the power generation of expensive power plants (due to the reduction of CHP power generation) and consequently increases the total operating cost of the system. In addition, the results show the impact of congestion of NG network pipelines on the unit commitment by increasing residential gas load. The impact of linepack technology on system operation was also evaluated. The results indicated that the application of linepack technology in the NG network increases flexibility and improves short-term operation. In addition, HES technology was used to absorb excess wind power and decreasing the operating cost of the integrated system. The application of an interval optimization approach is used to apply the uncertainty of wind power. In this approach, the single-objective uncertainty problem was transformed into a deterministic bi-objective problem with mean and deviation costs. The ϵ-constraint method and fuzzy approach were utilized to solve this bi-objective problem. The results show that by reducing cost deviation, the CSO incurs a higher average cost, making the integrated system more robust to the uncertainty of wind power. In general, the results showed that using the HES system, the operating costs of the non-gas-fired expensive unit reduces by 46.1%, and also the total operating costs of the integrated system reduces by 0.45%. Additionally, the presence of the linepack system in the natural gas network reduces the total operating costs of the system by 0.41%.

NOMENCLATURE

Acronyms

CHP	Combined heat and power
HES	Hydrogen energy storage
NG	Natural gas
H2P	Hydrogen to power
P2H	Power to hydrogen
GFPP	Gas-fired power plant
NGFPP	Non-gas-fired power plant
UC	Unit commitment
MILP	Mixed-integer linear programming

Index and sets

n,sp,u	Indices of NG nodes, and gas resources, fixed pressure points for the linearization of Weymouth equation
i,b,d	Indices of units, electric buses, electric demand
w,t,h	Indices of wind farms, scheduling time periods, HES
k	Index of extreme points in the feasible operating area of CHP unit
l,Tr	Set of NG network branches and power grid transmission lines
NK	Set of CHP unit extreme points
A_b^i	Set of power units i located at power grid bus b
A_b^d	Set of power grid demand d located at power grid bus b
A_b^h	Set of HES h located at power grid bus b
A_b^w	Set of wind power w located at the power grid bus b
A_n^{sp}	Set of NG producers sp located at NG network node n
CHP	Set of combined power and heat power plant
CU, GU	Set of the non-gas-fired and gas-fired power plant

Constants

H_t^{Load}	District heat load at period t
$P_{b,t}^{Load}$	Electricity demand of bus b at period t
P^K	Power generated corresponding to the k extreme point in the feasible operating area of CHP unit
Q^K	Heat generated corresponding to the k extreme point in the feasible operating area of CHP unit
ρ_b^{HES}	Generation mode cost of HES
$\eta_b^{P2H}, \eta_b^{H2P}$	Storage/Generation efficiency of HES system
$P_{b,Min}^{P2H}, P_{b,Min}^{H2P}$	Lower limits of the HES system
$P_{b,Max}^{P2H}, P_{b,Max}^{H2P}$	Upper limits of the of the HES system
A_b^{Max}, A_b^{Min}	Maximum/minimum capacity of HES system
XL	Power transmission network reactance
γ_p, γ_H	Energy consumption coefficients of CHP unit for energy production of electrical and heat
β_i	Energy consumption coefficients of GFPP i for energy production of electrical
P_i^{Max}, P_i^{Min}	Maximum/minimum power generated of unit i
R_i^{up}, R_i^{dn}	Ramp-up and ramp-down limit of unit i
T_i^{on}, T_i^{off}	Minimum on/ off time of power unit i
L_i^{on}/L_i^{off}	The number of hours that the power unit be on/off at the beginning of the time horizon
PW_w^{Max}	The maximum power generated of wind farmer w
f_b^{Max}	Transmission line capacity
$V_{sp}^{Max}, V_{sp}^{Min}$	Maximum/minimum of NG producer sp
$\mathrm{Pr}_n^{Max}, \mathrm{Pr}_n^{Min}$	Maximum/minimum pressure at node n
γ_{sp}^{gas}	Prices offered by NG producers sp
C_i^{GSU}, C_i^{GSD}	Startup/shutdown ramping limit of GFPPs i
C_i^{SU}, C_i^{SD}	Startup/shutdown ramping limit of NGFPP i
$PR_{n,u}/PR_{m,u}$	Constant pressure values u in pipeline nodes (n, m) of NG network for the linearization of Weymouth equation

Variables

$h_{n,m,t}$	Average mass of NG (linepack) in pipeline (n,m), at period t
$I_{b,t}^{P2H}, I_{b,t}^{H2P}$	Binary Storage/Generation status indicator HES system at period t
$I_{i,t}$	Binary variable commitment status of unit i at period t
$q_{n,m,t}$	Gas flow in pipelines (n,m), at period t
$P_{b,t}^{P2H}, P_{b,t}^{H2P}$	Storage/Generation hydrogen of the HES system at period t
$q_{n,m,t}^{in/out}$	Inflow/outflow NG rates of the pipeline (n,m), at period t
$f_{b,j,t}$	Power flow on line (b,j) at period t
$FC_{i,t}$	Fuel cost of NGFPP in unit i at period t
$Pr_{n,t}$	Pressure at node n, at period t
$y_{i,t}/z_{i,t}$	Startup/shutdown indicator for the unit i at period t, equal to 1 if unit i is turned ON/OFF at period t and 0 otherwise
$y_{n,m,t}$	Binary variable to ensure NG flow from node n to m or vice versa
$GSU_{i,t}/GSD_{i,t}$	Startup/shutdown of GFPP i at period t

$SU_{i,t}/SD_{i,t}$ Startup/shutdown cost of NGFPP i at period t
$A_{h,t}$ Stored hydrogen level of HES system at period t
$H_{i,t}$ The heat generated of the CHP unit at period t
$P_{i,t}$ The power output of generation unit i at period t
$PW_{w,t}$ The wind power output of the turbine w at period t
α_t^k Variable for representing the operating extreme points k of the CHP unit at period t
$V_{sp,t}$ NG producers sp at period t
$\delta_{b,t}$ Voltage angle at bus b and at period t

REFERENCES

1. Nazari-Heris, M., et al.: Combined heat and power economic dispatch problem solution by implementation of whale optimization method. Neural Comput. Appl. 31(2), 421–436 (2019)
2. Clegg, S., Mancarella, P.: Integrated modeling and assessment of the operational impact of power-to-gas (p2g) on electrical and gas transmission networks. IEEE Trans. Sustain. Energy 6(4), 1234–1244 (2015)
3. Zhang, X., et al.: Hourly electricity demand response in the stochastic day-ahead scheduling of coordinated electricity and natural gas networks. IEEE Trans. Power Syst. 31(1), 592–601 (2015)
4. Sheykhloei, B., et al.: Optimal co-scheduling of distributed generation resources and natural gas network considering uncertainties. J. Storage Mater. 21, 383–392 (2019)
5. Nazari-Heris, M., et al.: Economic-environmental effect of power to gas technology in coupled electricity and gas systems with price-responsive shiftable loads. J. Cleaner Prod. 244, 118769 (2020)
6. Zhang, Y., et al.: Cooperative optimization scheduling of the electricity-gas coupled system considering wind power uncertainty via a decomposition-coordination framework. Energy194, 116827 (2020)
7. Mirzaei, M.A., et al.: Integration of emerging resources in IGDT-based robust scheduling of combined power and natural gas systems considering flexible ramping products. Energy 189, 116195 (2019)
8. Zhang, X., et al.: Electricity-natural gas operation planning with hourly demand response for deployment of flexible ramp. IEEE Trans. Sustain. Energy 7(3), 996–1004 (2016)
9. Mirzaei, M.A., et al.: Stochastic network-constrained co-optimization of energy and reserve products in renewable energy integrated power and gas networks with energy storage system. J. Cleaner Prod. 223, 747–758 (2019)
10. Wang, X., et al.: Bi-level planning for integrated electricity and natural gas systems with wind power and natural gas storage. Int. J. Electr. Power Energy Syst. 118, 105738 (2020)
11. Qin, Y.J., et al.: Reduction of non-linear many objectives for coordinated operation of integrated energy systems. Int. J. Electr. Power Energy Syst. 117, 105657 (2020)
12. Bai, L., et al.: Interval optimization based operating strategy for gas-electricity integrated energy systems considering demand response and wind uncertainty. Appl. Energy 167, 270–279 (2016)
13. Sohrabi, F., et al.: Coordination of interdependent natural gas and electricity systems based on information gap decision theory. IET Gener. Transm. Distrib. 13(15), 3362–3369 (2019)
14. Mirzaei, M.A., et al.: A novel hybrid framework for co-optimization of power and natural gas networks integrated with emerging technologies. IEEE Syst. J. 14, 3598–3608 (2020)
15. Nasiri, N., et al.: A bi-level market-clearing for coordinated regional-local multi-carrier systems in presence of energy storage technologies. Sustain. Cities Soc. 63, 102439 (2020)
16. Hemmati, M., et al.: Optimal operation of integrated electrical and natural gas networks with a focus on distributed energy hub systems. Sustainability 12(20), 8320 (2020)
17. Li, Z., et al.: Combined heat and power dispatch considering pipeline energy storage of district heating network. IEEE Trans. Sustain. Energy 7(1), 12–22 (2015)
18. Aghaei, J., et al.: Optimal robust unit commitment of CHP plants in electricity markets using information gap decision theory. IEEE Trans. Smart Grid 8(5), 2296–2304 (2016)
19. Wang, H., et al.:Risk-averse market clearing for coupled electricity, natural gas and district heating system. CSEE J. Power Energy Syst. 5(2), 240–248 (2019)
20. Jiang, T., et al.: Optimal energy flow and nodal energy pricing in carbon emission-embedded integrated energy systems. CSEE J. Power Energy Syst. 4(2), 179–187 (2018)
21. Majidi, M., et al.: Optimal robust operation of combined heat and power systems with demand response programs. Appl. Therm. Eng. 149, 1359–1369 (2019)
22. Anand, H., Narang, N., Dhillon, J.S.: Multi-objective combined heat and power unit commitment using particle swarm optimization. Energy 172, 794–807 (2019)
23. Ali, A., Liu, N., He, L.: Multi-party energy management and economics of integrated energy microgrid with pv/t and combined heat and power system. IET Renewable Power Gener. 13(3), 451–461 (2018)
24. Aghaei, J., Alizadeh, M.-I.I.: Multi-objective self-scheduling of CHP (combined heat and power)-based microgrids considering demand response programs and ESSs (energy storage systems). Energy 55, 1044–1054 (2013)
25. Jabari, F., et al.: Optimal short-term coordination of water-heat-power nexus incorporating plug-in electric vehicles and real-time demand response programs. Energy 174, 708–723 (2019)
26. Marzoghi, A.F., et al.: Optimal scheduling of intelligent parking lot using interval optimization method in the presence of the electrolyser and fuel cell as hydrogen storage system. Int. J. Hydrog. Energy 44(45), 24997–25009 (2019)
27. Yu, D., et al.: Risk-averse stochastic operation of a power system integrated with hydrogen storage system and wind generation in the presence of demand response program. Int. J. Hydrog. Energy 44(59), 31204–31215 (2019)
28. Mirzaei, M.A., et al.: Stochastic security-constrained operation of wind and hydrogen energy storage systems integrated with price-based demand response. Int. J. Hydrog. Energy 44(27), 14217–14227 (2019)
29. Seyyedeh-Barhagh, S., et al.: Optimal scheduling of hydrogen storage under economic and environmental priorities in the presence of renewable units and demand response. Sustain. Cities Soc. 46, 101406 (2019)
30. Mehrjerdi, H.: Off-grid solar powered charging station for electric and hydrogen vehicles including fuel cell and hydrogen storage. Int. J. Hydrog. Energy 44(23), 11574–11583 (2019)
31. Bakhtiari, H., Naghizadeh, R.A.: Multi-criteria optimal sizing of hybrid renewable energy systems including wind, photovoltaic, battery, and hydrogen storage with constraint method. IET Renewable Power Gener. 12(8), 883–892 (2018)
32. Garciia-Triviño, P., et al.: Optimised operation of power sources of a pv/battery/hydrogen-powered hybrid charging station for electric and fuel cell vehicles. IET Renew. Power Gener. 13(16), 3022–3032 (2019)
33. Razipour, R., Moghaddas-Tafreshi, S-M., Farhadi, P.: Optimal management of electric vehicles in an intelligent parking lot in the presence of hydrogen storage system. J. Storage Mater. 22, 144–152 (2019)
34. Luo, L., et al.: Optimal scheduling of a renewable based microgrid considering photovoltaic system and battery energy storage under uncertainty. J. Storage Mater. 28, 101306 (2020)
35. Li, Z., et al.: Transmission-constrained unit commitment considering combined electricity and district heating networks. IEEE Trans. Sustain. Energy 7(2), 480–492 (2015)
36. Ordoudis, C., Pinson, P., Morales, J.M.: An integrated market for electricity and natural gas systems with stochastic power producers, Eur. J. Oper. Res. 272(2), 642–654 (2019)
37. Fodstad, M., Midthun, K.T., Tomasgard, A.: Adding flexibility in a natural gas transportation network using interruptible transportation services. Eur. J. Oper. Res. 243(2), 647–657 (2015)

38. Mohseni-Bonab, S.M., et al.: Voltage stability constrained multi-objective optimal reactive power dispatch under load and wind power uncertainties: A stochastic approach. Renew. Energy 85, 598–609 (2016)
39. Rabiee, A., et al.: Corrective voltage control scheme considering demand response and stochastic wind power. IEEE Trans. Power Syst. 29(6), 2965–2973 (2014)
40. Alabdulwahab, A., et al.: Stochastic security-constrained scheduling of coordinated electricity and natural gas infrastructures. IBM Syst. J. 11(3), 1674–1683 (2015)

How to cite this article: Nasiri N, Yazdankhah AS, Mirzaei MA, Loni A, Mohammadi-ivatloo B, Zare K, Marzband M. Interval optimization-based scheduling of interlinked power, gas, heat, and hydrogen systems. *IET Renew Power Gener.* 2021;15:1214–1226. https://doi.org/10.1049/rpg2.12101